# Ultra-Weak Fiber Bragg Grating OFDR Demodulation System Based on Adaptive Gaussian Fitting

LUO Zhihui1; YANG Xiangyu1; HUANG Jianglou1; RAN Changyan1; HUANG Bolin2; LI Jianzhi3; WANG Baochang1

*1. Hubei Engineering Research Center of Weak Magnetic-Field Detection, China Three Gorges University; 2. Hubei Key Laboratory of Disaster Prevention and Mitigation, China Three Gorges University; 3. Key Laboratory of Large-Structure Health Monitoring and Control, Shijiazhuang Tiedao University*

**Abstract:** To address the complex demodulation algorithms and limited real-time performance of ultra-weak fiber Bragg grating (UW-FBG) OFDR systems, this study develops an OFDR demodulation system based on adaptive Gaussian fitting. A power spectral density threshold is used to identify and locate UW-FBGs, and the 3σ criterion is introduced for dynamic trimming of the grating spectral interval, reducing the computational-resource demand of wavelength fitting. A 12-layer 250 MSPS system-on-chip board integrating high-speed acquisition, control, demodulation and communication is developed, and C# host software realizes grating-array localization, spectral analysis and demodulation. Experiments show that the developed OFDR system improves the speed by about 9.5 times compared with conventional wavelength demodulation. It achieves a maximum test distance of 100 m, a spatial resolution of 0.16 mm, temperature measurement accuracy up to ±0.1 °C, power consumption below 22 W and dimensions of 234 mm x 180 mm x 45 mm, providing a cost-effective solution for OFDR engineering applications.

**Keywords:** optical frequency domain reflectometry; ultra-weak fiber Bragg grating; adaptive Gaussian fitting algorithm; field-programmable gate array; modularization

## Figure and Table Captions



## 1. Introduction

Optical frequency domain reflectometry (OFDR) is a fiber-sensing technique for continuous distributed detection of temperature and other physical quantities based on backward Rayleigh scattering. Its spatial resolution can reach the millimeter or even micrometer level, which gives it broad prospects in shape reconstruction and structural damage identification.

Conventional OFDR systems usually use ordinary single-mode fiber as the sensing element. The backward Rayleigh scattering has poor directionality and weak intensity, so the sensing signal is susceptible to source nonlinearity, phase noise and other factors. System accuracy and dynamic range are therefore limited. Ultra-weak FBG arrays improve reflection intensity and directionality by inscribing large numbers of FBGs with reflectivity below 0.1% in ordinary fiber, significantly improving system performance and becoming a research focus for new OFDR systems.

Current UW-FBG OFDR systems commonly adopt cross-correlation algorithms for demodulation. However, cross-correlation can suffer from false peaks caused by noise, spatial-resolution degradation, spatial mismatch under large-strain conditions and excessive time-frequency data volume, limiting real-time performance. Simplifying UW-FBG OFDR demodulation algorithms is therefore necessary.

Wavelength demodulation is accurate and reliable and is widely used in FBG and UW-FBG sensing. However, it requires complete spectral data for each grating. As the number of gratings increases, computational requirements rise sharply. In OFDR systems, mm-level resolution requires a much higher density of UW-FBGs. If full-spectrum demodulation is used, large resource consumption severely limits real-time response and instrument miniaturization. Existing commercial OFDR systems are often large and inconvenient for field applications, while domestic instruments still face challenges in size and power consumption.

In response, this paper proposes an UW-FBG OFDR demodulation system based on adaptive Gaussian fitting. By analyzing PSD characteristics of UW-FBGs, the system uses a dynamic threshold to identify and locate gratings and applies the 3σ criterion to trim grating spectra, thereby reducing the computational cost of wavelength fitting. A modular system based on SoC hardware is developed to improve the engineering suitability of OFDR.

## 2. Working Principle of the UW-FBG OFDR System

In the UW-FBG OFDR system, light from a tunable laser is divided by a coupler into two paths. One path enters an auxiliary interferometer to generate an interference signal as a compensation reference. The other path enters the main interferometer, where the UW-FBGs sense external changes and beat with the reference arm of the main interferometer. Backscattered or reflected signals from different positions reach the photodetector at different times and generate beat signals with different frequencies.

The theoretical spatial resolution is limited by the laser sweep range, while the maximum effective measurement distance is limited by both the sampling rate and sweep rate. Thus, OFDR system performance depends strongly on source sweep range, sweep speed and acquisition bandwidth.

## 3. Adaptive Gaussian Fitting Algorithm

UW-FBGs are used as sensing units, and their reflection peaks appear as discrete and easily identifiable characteristic peaks in the OFDR frequency-domain spectrum. Because grating spacing may vary, automatic grating identification is required. After preprocessing the UW-FBG reflection signal, the mean PSD is calculated and a dynamic threshold is defined. When the PSD amplitude remains above this threshold for a minimum number of consecutive sampling points corresponding to one complete grating region, the segment is identified as a UW-FBG unit. Traversing the distance domain then determines the grating positions.

The spectrum of each grating can be recovered through IFFT. Similar to ordinary FBG spectra, a single UW-FBG reflection spectrum can be described by a Gaussian function. Taking the natural logarithm of spectral data and fitting the Gaussian function by least squares yields the optimized center wavelength.

Because Gaussian fitting complexity increases with the square of the number of fitting points, identifying the optimal fitting region is essential for improving demodulation speed while preserving accuracy. The 3σ criterion indicates that about 99.73% of the energy of a Gaussian distribution lies within the interval [μ - 3σ, μ + 3σ]. Therefore, fitting can be limited to this region to accurately analyze the Bragg peak wavelength.

Under a sampling rate of 50 MSPS, sweep range of 5 nm and sweep rate of 20 Hz, dynamic trimming shows that the retained 6σ spectral characterization region accounts for only about 6.5%-14.5% of the complete spectrum, reducing the data volume by nearly one order of magnitude compared with conventional algorithms.

## 4. Software and Hardware Implementation

The UW-FBG OFDR demodulation module uses an aluminum-machined enclosure with external heat dissipation, a 12 V DC power supply, total power consumption below 22 W and dimensions of 234 mm x 180 mm x 45 mm. The module integrates a swept source, optical path structure and embedded signal acquisition/processing board.

The hardware core uses a Zynq7100 system-on-chip integrating ARM and FPGA circuits. The FPGA is responsible for light-source control, high-speed synchronous acquisition, data buffering, computation and frame formation. The ARM implements high-speed data exchange with the host computer through Gigabit or 10 Gigabit Ethernet. A 12-layer multifunction board was independently developed. For domestic substitution, the FPGA and high-speed A/D chips use domestic alternatives. The swept source is an ITXL-03 device with a 5 nm sweep range, 20 Hz sweep rate and 300 kHz linewidth.

The host computer interface is written in C# and includes the distance-domain reflection plot, single-grating spectrum plot, factory settings and regional temperature/strain test functions. The distance-domain plot shows UW-FBG positions in real time. The single-grating spectrum plot uses a cursor to select a sensing unit and display its spectral variation. The regional test function senses temperature or strain in a selected zone.

## 5. OFDR System Performance Test and Analysis

### 5.1 Experimental Platform

The test system places part of the UW-FBG sensing array in a water-bath heating device and connects it to the OFDR module. The module is connected to a notebook computer by Gigabit Ethernet and powered by a programmable power supply. The UW-FBGs have a center wavelength of 1554 nm, grating length of 5 mm, spacing of 5 mm, 3 dB bandwidth of 0.21 nm and reflectivity of 0.1‰-1‰. The actual system power consumption was measured as 21.209 W.

After the UW-FBG array was connected, the measured maximum distance was 100 m, consistent with the theoretical value. The frequency width of the fiber end corresponded to a spatial resolution of 0.16 mm, also consistent with theory.

### 5.2 Demodulation Speed

Continuous acquisition was performed under stable conditions. The same signal was demodulated using cross-correlation, conventional wavelength demodulation and adaptive Gaussian fitting. The three methods had similar accuracy, but the adaptive Gaussian fitting algorithm required an average of only 1.022 ms. This is about 56.5 times faster than cross-correlation at 57.769 ms and about 9.5 times faster than conventional wavelength demodulation at 9.66 ms.

### 5.3 Temperature Sensing Characteristics

A 1.55-1.60 m section of the 5 mm dense UW-FBG array, containing five grating points, was immersed in a water bath and heated from 23 °C to 26 °C. The waterfall plot showed clear center-wavelength shifts for the temperature-changing region. In another test, the heated zone was changed to UW-FBG #14-#23, and the temperature was increased to 53 °C in steps of 3 °C. The selected grating segment showed obvious wavelength shifts while other grating points remained stable.

For UW-FBG #15, the spectral shape shifted with temperature and the relationship between center-wavelength shift and temperature was linear with $R^2 = 0.99896$. Comparison between the host-computer temperature output and a platinum thermometer showed an error of approximately ±0.01 °C relative to the platinum thermometer, confirming measurement accuracy up to ±0.1 °C.

## 6. Conclusion

This paper proposes and validates a UW-FBG OFDR demodulation system based on adaptive Gaussian fitting. PSD thresholding is used for grating localization, and the 3σ criterion dynamically trims the spectral fitting interval. The algorithm improves speed by about 9.5 times over conventional wavelength demodulation and 56.5 times over cross-correlation. The domestic OFDR system achieves a temperature-sensing linearity of 0.99896, accuracy of ±0.1 °C, dimensions of 234 mm x 180 mm x 45 mm and power consumption below 22 W. Core optical-source and electronic components are domestically substitutable, providing a practical solution for OFDR application and promotion.

## Translated Tables

Table 1. Comparison of adaptive fitting-point numbers for different UW-FBGs

| UW-FBG type | FWHM 0.13 nm | FWHM 0.29 nm |
|---|---|---|
| Center wavelength 1554 nm | 81243 | 181247 |
| Center wavelength 1552 nm | 81254 | 181252 |

Table 2. Demodulation algorithm uncertainty and time comparison

| Algorithm | Measurement uncertainty (pm/time) | Average computation time (ms/time) |
|---|---|---|
| Cross-correlation | ±2.492 | 57.769 |
| Conventional wavelength demodulation | ±3.371 | 9.66 |
| Adaptive Gaussian fitting | ±1.986 | 1.022 |

Table 3. Temperature measurement comparison between the OFDR module and platinum thermometer

| Measurement | OFDR module (°C) | Platinum thermometer (°C) |
|---|---|---|
| Temp1 | 22.79 | 22.79 |
| Temp2 | 25.63 | 25.64 |
| Temp3 | 28.89 | 28.89 |
| Temp4 | 31.78 | 31.77 |
| Temp5 | 34.21 | 34.22 |
| Temp6 | 37.58 | 37.59 |
| Temp7 | 40.36 | 40.37 |

| | | |
|---|---|---|
| Temp8 | 43.67 | 43.69 |
| Temp9 | 46.42 | 46.42 |
| Temp10 | 49.50 | 49.49 |

## References

*Reference entries are retained in the original citation form to avoid altering source bibliographic data.*


LV Y J, LI H, AI K, et al. Ultra-High Resolution φ-OFDR Strain Sensor Based on BEOF and PMC-OPC Scheme[J]. Journal of Lightwave Technology, 2025, 43(5): 2363-2370.

DING Z Y, GUO H H, LIU K, et al. Advances in Distributed Optical Fiber Sensors Based on Optical Frequency-Domain Reflectometry: A Review[J]. IEEE Sensors Journal, 2023, 23(22): 26925-26941.

朱坤垚, 江毅. 光频域反射计研究进展[J]. 激光与光电子学进展, 2024, 61(05): 23-39.

唐轶, 冯智宇, 成煜, 等. 基于光频域反射计的分布式传感及复合传感研究进展[J]. 激光与光电子学进展, 2024, 61(15): 33-44.

YANG M, BAI W, GUO H, et al. Huge capacity fiber-optic sensing network based on ultra-weak draw tower gratings[J]. Photonic Sensors, 2016, 6(1): 26-41.

LEE X, CHE Q, LIU X, et al. Effects of weak fiber Bragg gratings on a distributed vibration sensing system based on phase-sensitive optical time-domain reflectometry[J]. Optical Engineering, 2019, 58(08): 087103.

ZHANG H, FAN D, MA Y, et al. Interrogation of 5000 ultraweak fiber Bragg grating sensors using optical frequency domain reflectometry[J]. Optical Engineering, 2018, 57(10): 106110.

PENG Z W, SHI Y B, SUI R L, et al. Multi-Channel OFDR Strain Sensor Based on Wavelength/Space Division Multiplexing Weak FBG Arrays[J]. Journal of Lightwave Technology, 2025, 43(17): 8492-8497.

ZOU D J, SONG Z, LIANG C P, et al. Distributed ultra large strain measurement range sensing based on spectral shift adjacent point difference method in OFDR[J]. Optics and Laser Technology, 2024, 176: 111003.

LIU K J, YIN G L, LOU Y Y, et al. Optical frequency domain reflectometer based on spectral segmented normalized cross correlation[J]. Optics & Laser Technology, 2025, 191.

吴紫航, 刘庆文, 何祖源. 光频域反射仪高精度快速频谱解调算法[J/OL]. 激光与光电子学进展, 2025: 1-16[2025-10-20].https://link.cnki.net/urlid/31.1690.TN.20250818.0958.002.

杨志, 鞠婉秋, 李永倩. FBG 波长高精度解调的研究进展[J]. 光通信技术, 2021, 45(03): 4-9.

YAO G Z, YIN Y M, LI Y Q, et al. High-precision and wide-wavelength range FBG demodulation method based on spectrum correction and data fusion[J]. Optics express, 2021, 29(16): 24846-24860.

江虹, 郭宇龙, 郑晓丹, 等. 一种改进的高精度光谱寻峰算法研究[J]. 光通信研究, 2020, (01): 33-37.

李政颖, 孙文丰, 王洪海. 基于光频域反射技术的超弱反射光纤光栅传感技术研究[J]. 光学学报, 2015, 35(08): 64-71.

LUNA Innovations. Optical Distributed Sensor Interrogators 7100 Datasheet[Z]. 2025.

刘庆文. 双边带光频域反射仪: 202210559130.3[P]. 2023-03-14.

董永康. 一种基于散射增强点位置偏移补偿的光纤应变解调方法及系统: 202510479176.8[P]. 2025-04-16.

盛骤, 谢式千, 潘承毅. 概率论与数理统计[M].北京: 高等教育出版社, 2008.



作者简介:

罗志会（1975—），副教授，博士，主要研究领域为超弱光纤光栅阵列传感技术及应用。E-mail:zhihui_luo@126.com

杨翔宇（2000—），硕士研究生，主要研究方向为结合超弱光纤光栅阵列的光频域反射传感技术。E-mail:y719779137@163.com


## Retained Figures and Visual Materials

*The original figures, screenshots, diagrams and experimental plots from the source manuscript are retained below in their original order for layout continuity. Captions in the translated body follow the source numbering where available.*

**Original visual material 1**

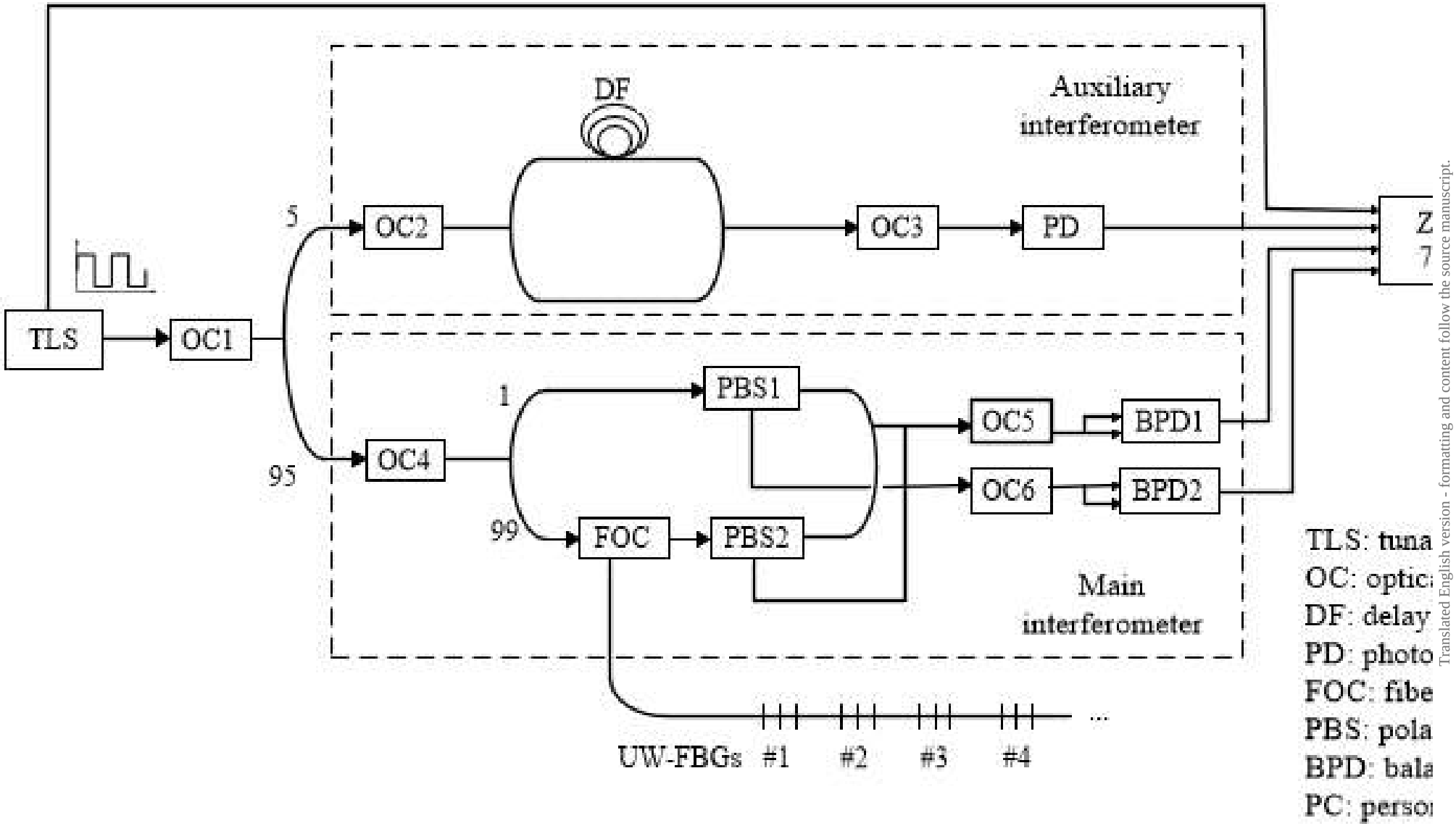

**Original visual material 2**

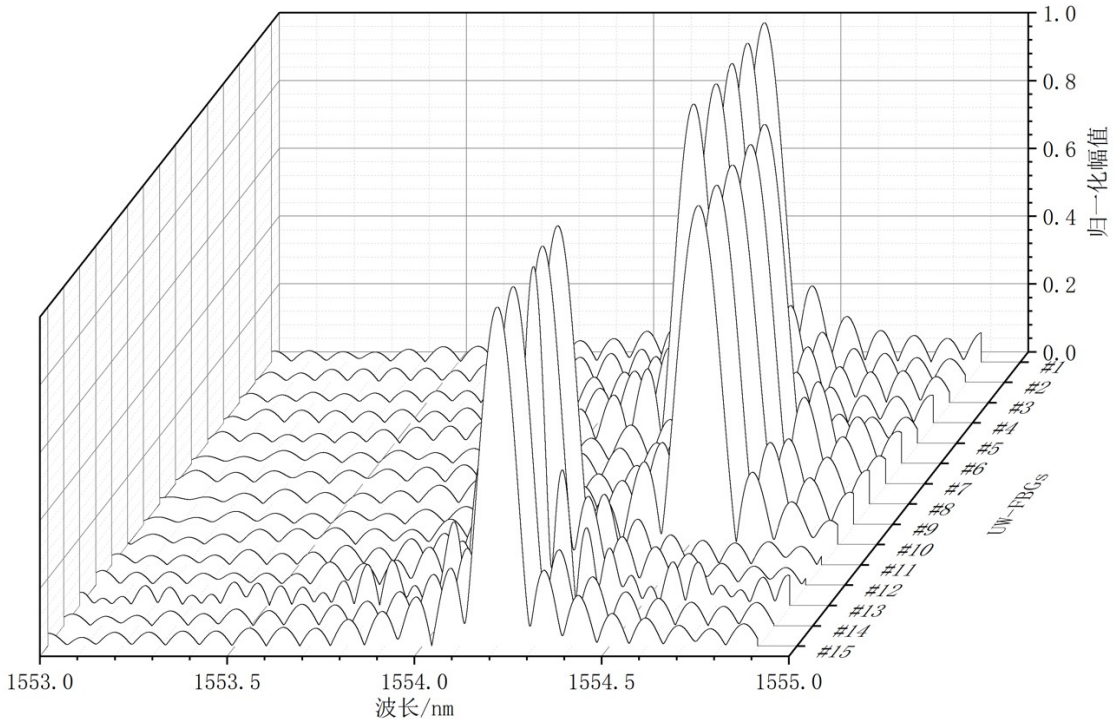


**Original visual material 3**

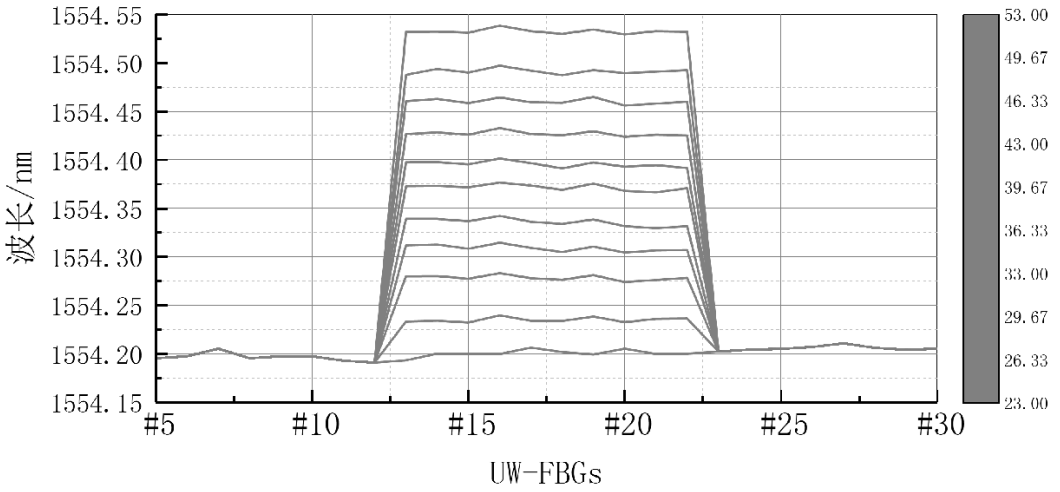


**Original visual material 4**

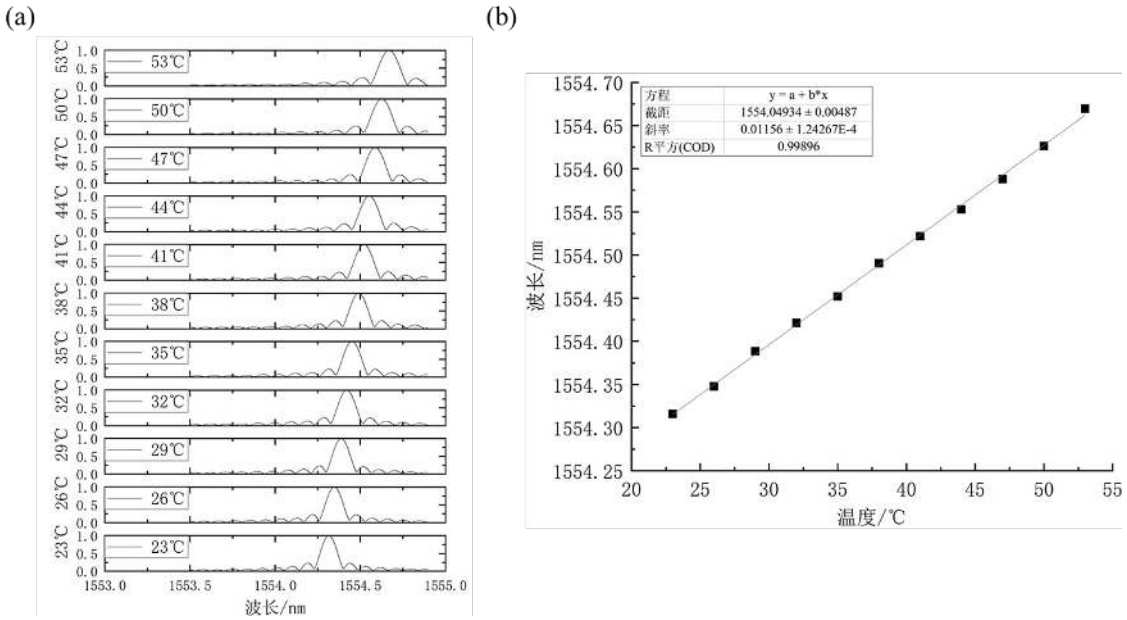


**Original visual material 5**

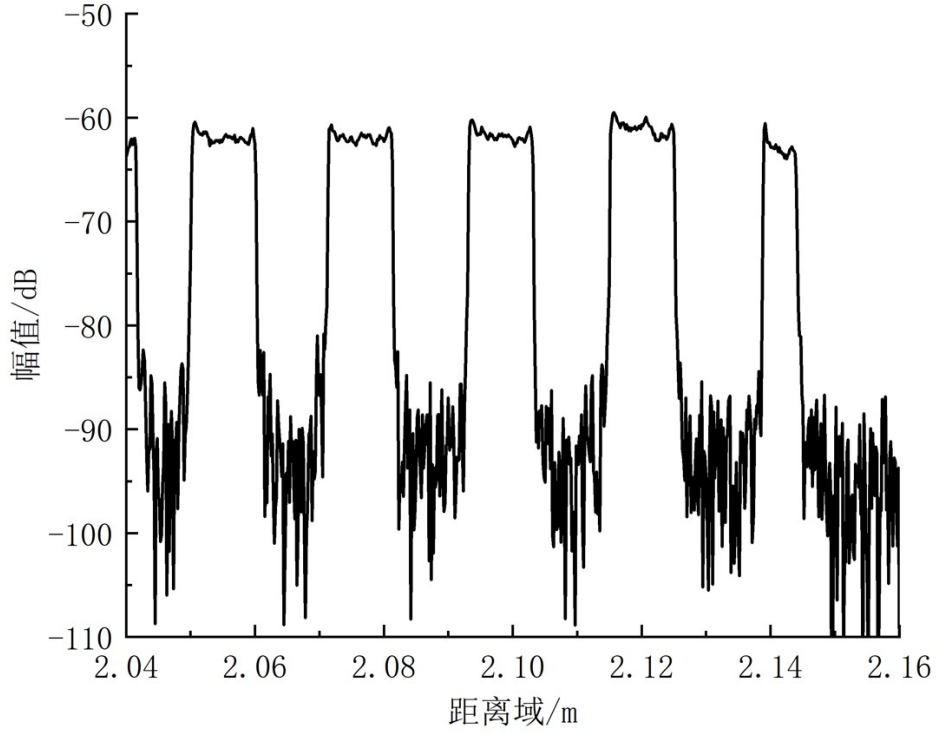


**Original visual material 6**

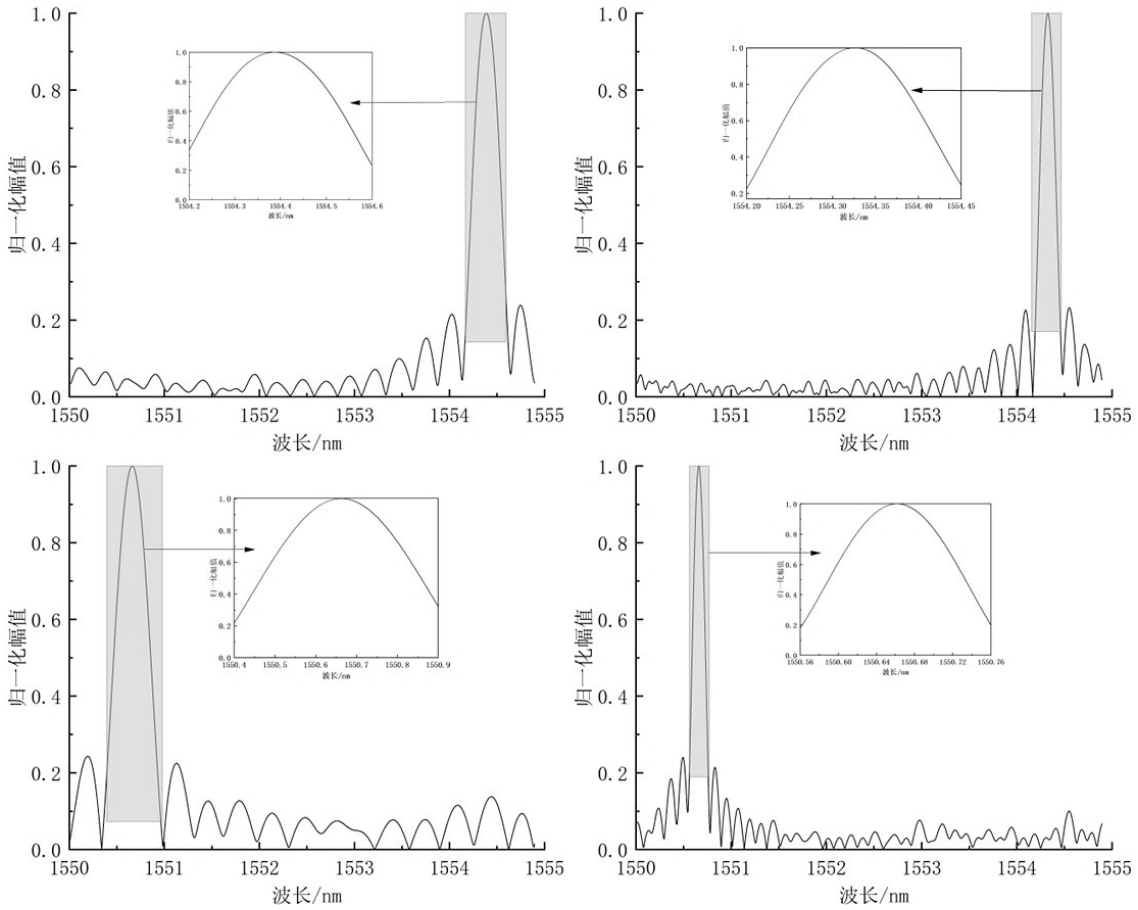


**Original visual material 7**

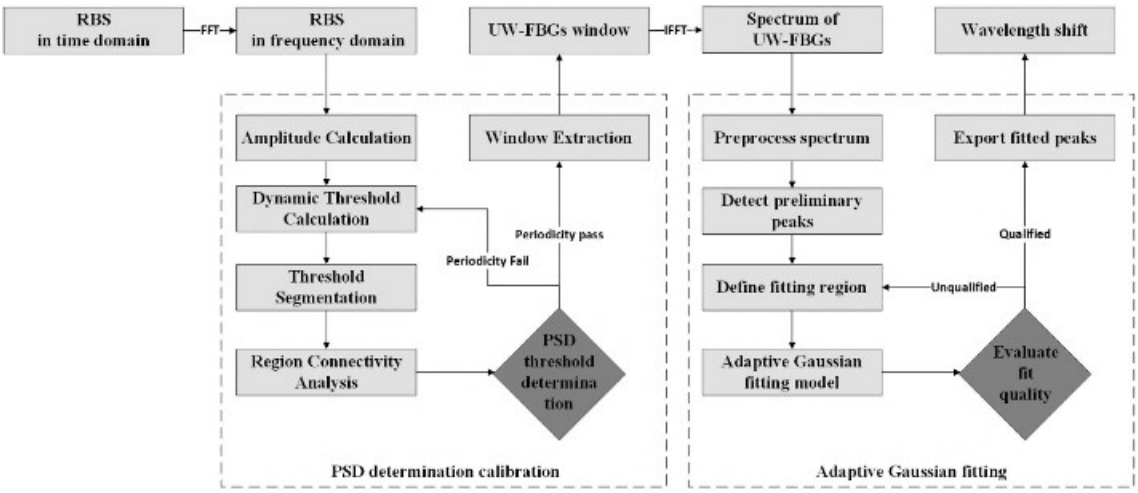


**Original visual material 8**

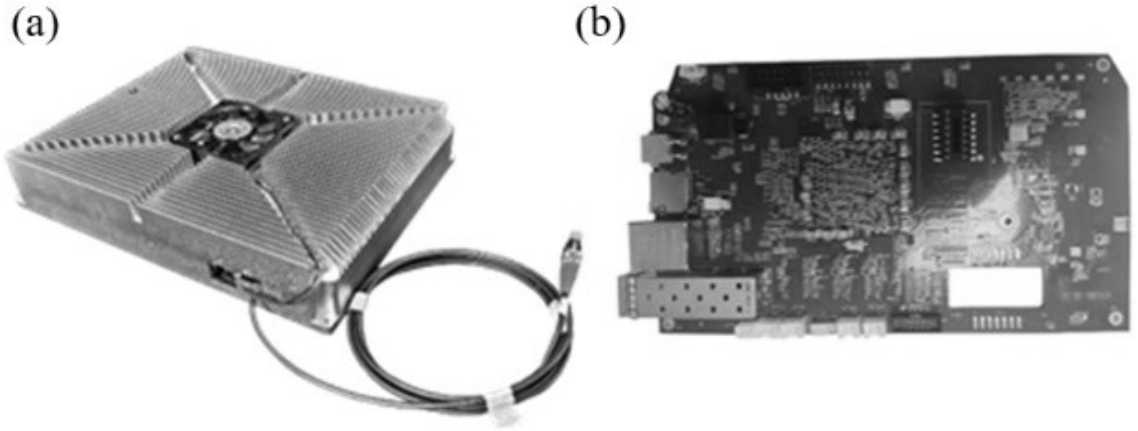


**Original visual material 9**

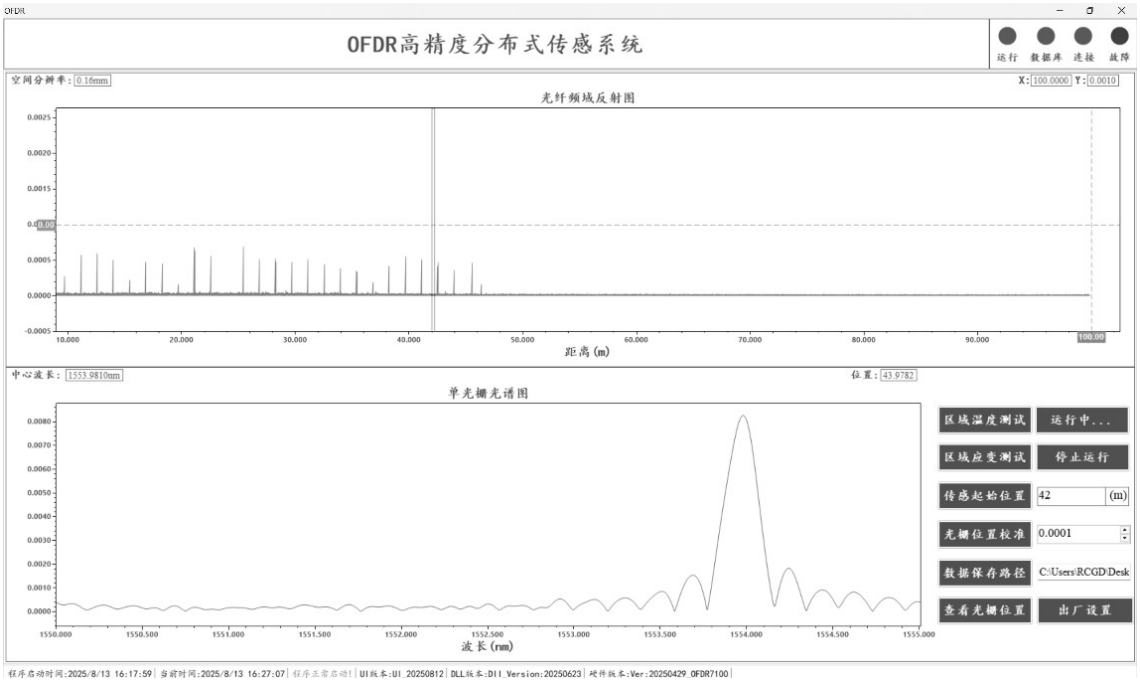


**Original visual material 10**

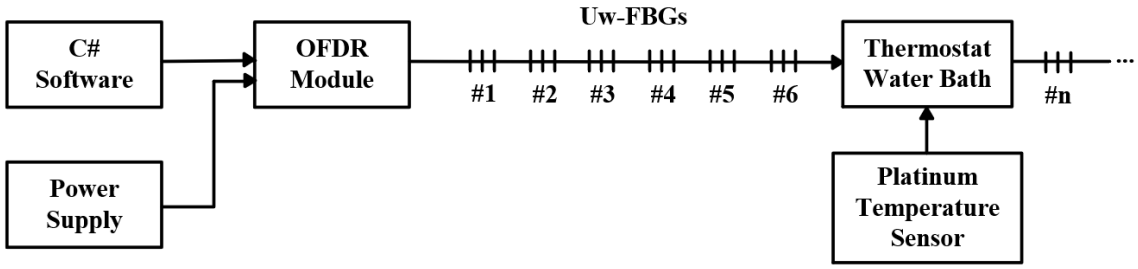


**Original visual material 11**

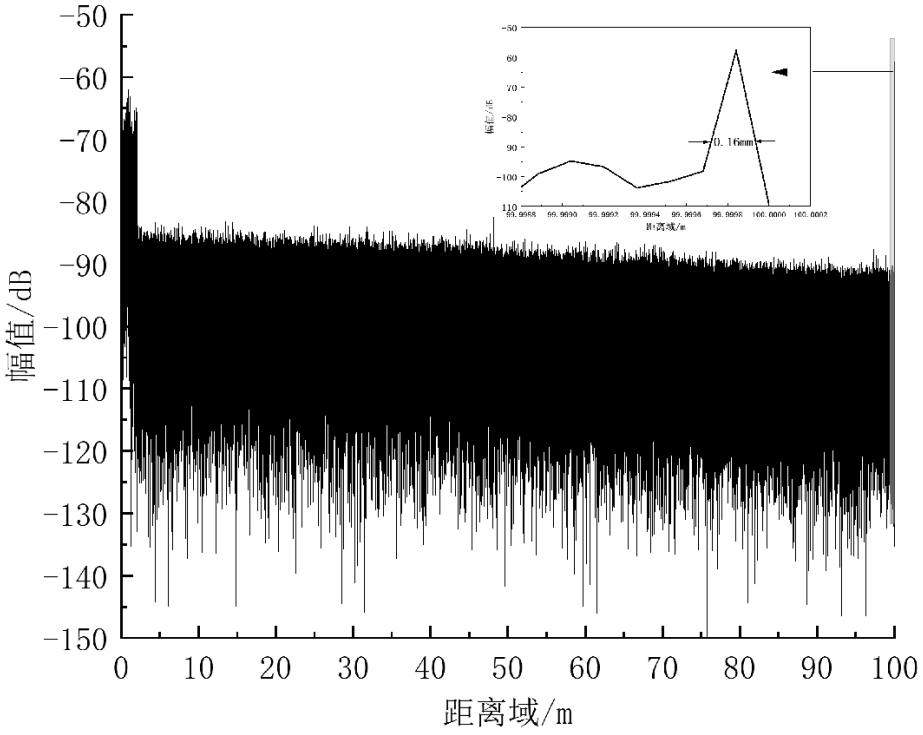


**Original visual material 12**